EFFECT OF MICROSTRUCTURE ON THE CYCLIC RESPONSE AND FATIGUE BEHAVIOR OF AN XD™ ALUMINUM METAL MATRIX COMPOSITE

G. M. Vyletel, D. C. Van Aken, and J. E. Allison*
Department of Materials Science and Engineering, The University of Michigan, Ann Arbor, MI 48109-2136
*Research Staff, Ford Motor Company, Dearborn, MI 48121

Introduction

Particulate reinforced metal matrix composites are being viewed with increasing interest by designers of high performance components. These composites offer many advantages over their unreinforced counterparts and provide the designers with increased flexibility in tailoring the material's properties, e.g. coefficient of thermal expansion and elastic modulus. However, these components are often employed in fatigue limited applications and to date there are only a few studies on the fatigue crack initiation behavior of metal matrix composites (e. g. 1-3). In particular, the cyclic stress - strain response of composite materials has not been documented nor has the influence of matrix microstructure on fatigue life or cyclic response been explored. Thus the purpose of this work was to investigate the effect of microstructure on the fatigue life, cyclic response, and strain localization of an aluminum-copper based XD™ particulate reinforced metal matrix composite. Since aluminum-based metal matrix composites are often based on conventional precipitation hardened aluminum alloys, an understanding of the fatigue behavior of these alloys provides a foundation for understanding the response of composite materials when subjected to cyclic loading. Of particular interest are comparisons between the fatigue behavior of materials hardened with either shearable or nonshearable precipitates. For comparison with the present work on cyclic response the reader is referred to the works of Laird and coworkers (e.g. 4-6).

Experimental Procedure

The material used in this study was prepared by AMAX R&D, Golden, Colorado. An aluminum metal matrix composite with 15 volume percent TiC was produced via the XD™ process (7) and subsequently direct chill cast. The matrix composition was similar to the commercial aluminum alloy 2219; however, the standard grain refining elements Zr, V, Ti were not added. The composition of the matrix is given in Table I. After casting, the material was extruded into 15.8 mm cylindrical bar stock with a final extrusion ratio of 27:1.

The composite was solution treated at 535° C for 4 hours followed by an ice water quench. Subsequent aging treatments were performed to obtain two different types of strengthening precipitates. A room temperature (natural) age of at least 400 hours was chosen to produce a microstructure consisting of shearable Guinier-Preston (GP) zones and an artificial aging temperature of 190° C was chosen to produce a microstructure consisting of nonshearable θ' precipitates. The peak aging time at 190° C was found to be 12 hours. Both hardness studies and tensile tests were used to establish the peak aging heat treatment. The tensile properties of these two microstructures are shown in Table II.

Uniaxial fatigue tests were performed on cylindrical samples with a gage length of 12.7 mm and a gage diameter of 5.1 mm under two testing conditions: 1.) load control (LC) with a load ratio (R) of -1 and a test frequency of 40 Hz and 2.) plastic strain control (PSC) at a test frequency of 1 Hz. The samples were machined using a low stress grinding procedure to minimize residual surface stresses. The presence of the reinforcing particulate precluded electro-

Table I. Composition of XD™ 2219 15% TiC

Element	Cu	Mn	V	Zr	Mg	Si	Fe
wt %	6.28	0.3	0.01	0.008	0.03	0.03	0.05

Table II. Tensile Properties of XD™ 2219 15% TiC

	Nat. Aged	Art. Aged
Yield Strength (MPa)	181	374
Tensile Strength (MPa)	337	446
Uniform Elongation (%)	15	5.5
Plastic Elongation (%)	19.5	8.8

polishing of the samples and hence the samples were tested in the low stress ground condition. All testing was micro-processor controlled and performed in a 44 kN servo-hydraulic test system with a precision aligned gripping fixture.

Results

The XD™ process produced an even distribution of spherical TiC particles in the aluminum matrix. The average particle size of the TiC particulate was 3.3 μm with a standard deviation based upon a normal distribution of ± 1.7 μm. As a result of the XD™ process, Al_3Ti intermetallics were also present with a measured volume fraction of 0.01 ± 0.004. These Al_3Ti particles existed as rods with an average length of 53.4 μm ± 26.7 μm and an average diameter of 10.2 μm ± 3.8 μm. Figure 1 shows a typical cross section of the material used in this investigation. Metallographic samples were electrolytically etched using Barker's reagent. A grain size of 23 ± 4.2 μm was measured by a linear intercept method transverse to the extrusion direction.

For the naturally aged material, the GP zones were unresolvable using conventional transmission electron microscopy. High resolution imaging of the naturally aged material, using a JEOL 4000EX operating at 300 keV, is in progress and initial studies indicate that the GP zone size is on the order of one monolayer thick and 3.0 nm in diameter. In addition, constituent particles (less than 1μm in diameter) were observed in both the naturally and artificially aged materials. These constituent particles contained Al, Cu, and Mn with a Cu:Mn ratio varying between 1:1 and 2:1. These constituent particles are believed to be $Al_{20}Mn_3Cu_2$ as predicted by the ternary phase diagram (8). Transmission electron microscopy of the artificially aged samples showed that the microstructure consisted of coarse θ' and regions consisting of both θ' and θ". The coarse θ' was often associated with the area adjacent to the reinforcing TiC particulate. Figures 2a and 2b show the typical microstructure of the naturally aged and artificially aged condition, respectively.

Under constant plastic strain amplitude testing, the naturally aged material exhibited two regimes of hardening. For plastic strain amplitudes greater than 1.0×10^{-3}, the typical cyclic response consisted of a rapid cyclic hardening regime followed by a regime termed "secondary hardening" in which the hardening continued until failure but at a considerably lower rate. The rapid hardening stage comprised approximately 7.0% of the total life of the sample. For plastic strain amplitudes less than or equal to 1.0×10^{-3}, rapid cyclic hardening and secondary hardening were observed followed by cyclic softening. This softening was observed in both the tensile and compressive maxima. In contrast, peak stresses in the artificially aged material reached a stable level within the first few cycles and remained at this saturation stress until failure. This behavior was observed over the entire range of plastic strain amplitudes tested. Figure 3 shows the typical cyclic response of these two microstructures. For plastic strain amplitudes less than 5×10^{-3}, the naturally aged material cyclically hardened to a higher saturation stress than did the artificially aged material. At higher plastic strain amplitudes the same nominal saturation stress was attained for both heat treated conditions.
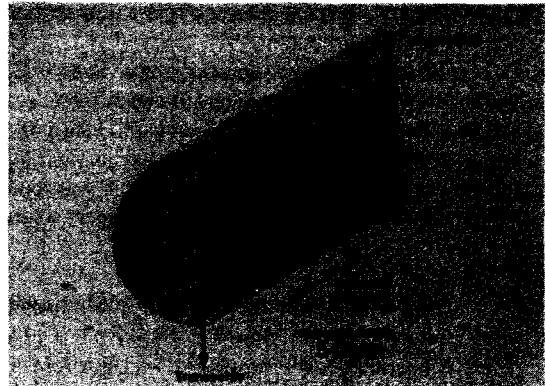

Figure 1. Typical microstructure of XD™ 2219 with 15 volume percent TiC.
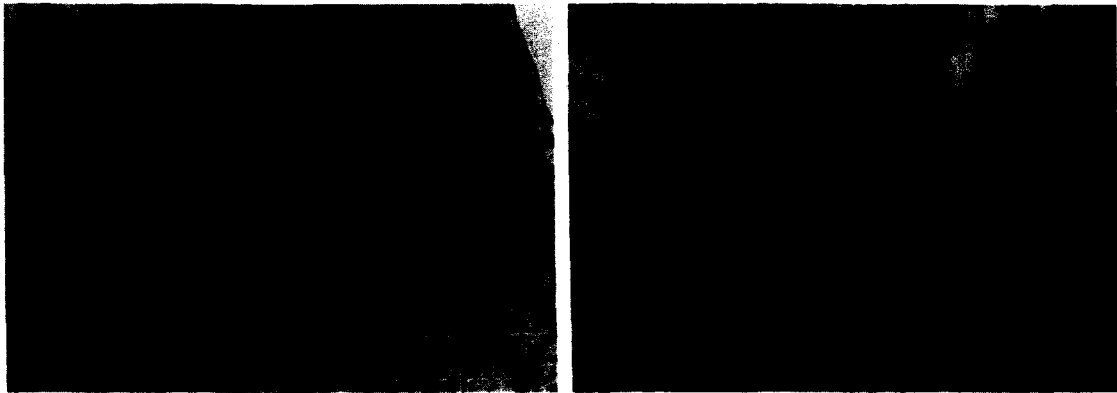
Figure 2. a) Bright-field transmission micrograph of the naturally aged microstructure showing constituent particles. b) Bright-field transmission micrograph of artificially aged material.

In the current study, the as-ground surface finish precluded direct surface observation of persistent slip band formation; thus a loop shape analysis as proposed by Mughrabi (9) and further developed by Witmer et al.(10) was performed to determine the extent of strain localization. The loop shape parameter has been defined as the area inside the stress-strain hysteresis loop divided by the area of a circumscribed parallelogram. A more detailed explanation of the loop shape analysis employed here may be found in reference 10. At plastic strains less than 1.0×10^{-3}, the loop shape analysis of the naturally aged material showed a distinct minimum which may be interpreted as the start of strain localization, i.e. the formation of PSBs. At larger plastic strain amplitudes, no significant change in the loop shape parameter was evident. For the artificially aged material, there was no change in the loop shape parameter throughout the life of the test. Figure 4 shows the loop shape parameter (V_H) as a function of the number of reversals for both naturally aged and artificially aged microstructures fatigued at a plastic strain amplitude of 2.5×10^{-4}.

Although the cyclic response of these two microstructures was markedly different, the strain-controlled fatigue life of these materials was nearly identical. Figure 5 shows a Coffin-Manson plot of the naturally aged and artificially
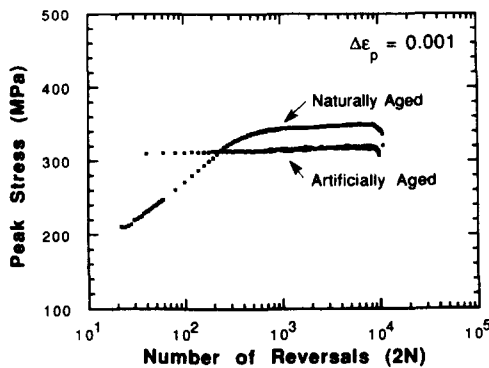

Figure 3. Typical cyclic response of XD™ 2219 15% TiC naturally aged and artificially aged microstructures. The plastic strain amplitude was $\Delta\varepsilon_p = 0.001$.
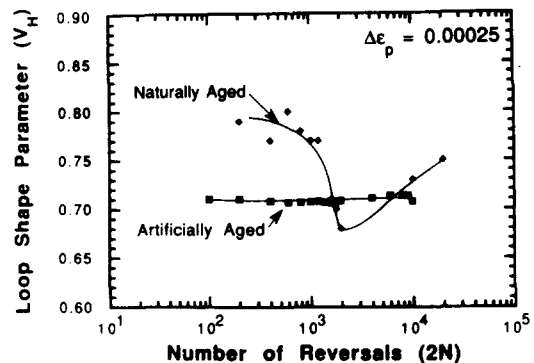
Figure 4. Variation in loop shape parameter as a function of number of cycles for naturally and artificially aged microstructures.
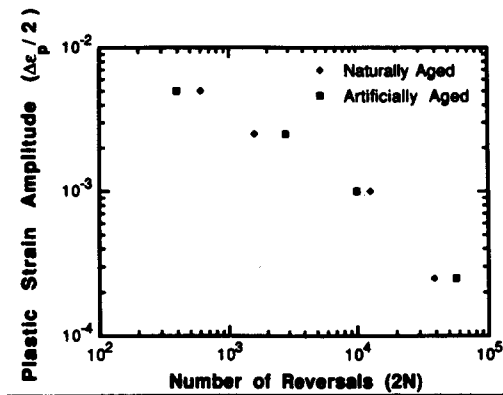
Figure 5. Coffin - Manson plot of data from artificially aged and naturally aged microstructures.
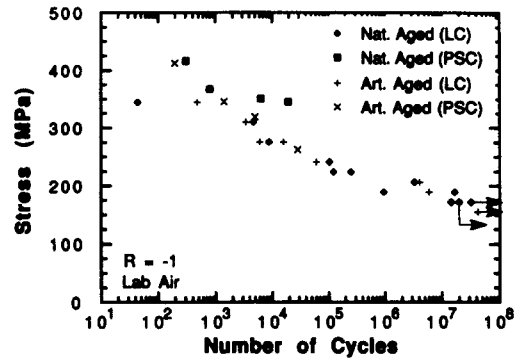
Figure 6. S - N plot of XD™ 2219 15% TiC. Both naturally aged and artificially aged microstructures show the same fatigue lives for life times greater than 1×10^5. Load control (LC) and plastic strain control (PSC) data are plotted on this curve.

aged materials. Furthermore, Figure 6 shows that the load control fatigue data yields virtually identical S-N curves for samples with a life greater than 3×10^3 cycles. Also plotted in Figure 6 are the peak stresses from the plastic strain-controlled tests. For the artificially aged samples, the plastic strain control data was in good agreement with the data from the load control tests.

Discussion

The microstructures observed in this study were typical of those observed by Papazian (11). The nonuniform distribution of θ' and θ" observed in the artificially aged microstructure for the present study is typical of what is observed for wrought 2219-T6 aluminum alloys. Papazian (11) has shown that the distribution of θ' and θ" in these artificially aged wrought alloys can be dependent upon prior mechanical treatment. Stretching the material prior to the aging treatment will produce a more uniform size and distribution of θ' precipitates. Papazian also demonstrated that the nonuniform distribution of θ' observed in 2219-T62 was eliminated by the stretching operation used in the processing of 2219-T87. In this context the nonuniform precipitates observed in the present study may be explained. It is known that a high dislocation density in the vicinity of the particulate reinforcement may be created by the thermal expansion mismatch between TiC and the aluminum matrix. Thus, the coarse θ' precipitates observed near the TiC reinforcement can be attributed to a higher dislocation density near the TiC particulate reinforcement.

The cyclic hardening behavior of the naturally aged microstructure was similar to the behavior observed by Calabrese and Laird (4) for Al-4Cu aged to contain θ", with the exception that they did not observe the "secondary hardening" region in their study. This may be due to differences in the cyclic response between microstructures containing θ" and microstructures containing GP zones or possibly an effect of a fine grain size in the composite material. Similar behavior was observed in an unreinforced commercial alloy, 2024-T351 by Sanders et al (12). The rapid hardening region of the cyclic hardening curve is believed to be related to dislocation multiplication and dislocation-precipitate interactions. As the dislocation density increases, the stress required to obtain the desired plastic strain amplitude is thus increased. However, the mechanism associated with the secondary hardening is yet unclear and further work is needed. It is presumed that the softening mechanism just prior to failure is related to the dissolution of the GP zones as they are cut by dislocations within the PSBs. For plastic strains greater than 1.0×10^{-3}, no cyclic softening was observed in the composite. This may be explained by the activation of secondary slip systems at higher plastic strain levels which would tend to homogenize slip. It should be noted that Santner and Fine observed somewhat different behavior in two binary Al-Cu alloys in the naturally aged condition (13). However, they tested at strains which were generally larger than those used in the current study.

For the naturally aged samples fatigued at a plastic strain amplitude of 2.5×10^{-4}, the loop shape parameter

continually decreased to a minimum then started to increase. Both Witmer et al.(10) and Polak et al.(14) have shown that a minimum in the loop shape parameter corresponds to the nucleation of PSBs. The presence of PSBs has been confirmed in this material by TEM. From Figure 4, the minimum in loop shape parameter for the naturally aged material occurred after the transition from rapid hardening to secondary hardening occurred in the cyclic hardening curve. Increasing the applied plastic strain on the naturally aged composite diminished the distinct minimum in the loop shape parameter. This is similar to the results of Polak et al. (14) where large plastic strain amplitudes tend to eliminate any dramatic changes in the loop shape parameter. The lack of a minimum at higher plastic strain amplitudes may be caused by the activation of secondary slip systems. In addition, polycrystalline materials tend to decrease the magnitude of change in the loop shape parameter (14) and this should be accentuated by the fine grain size observed for the composite material.

The artificially aged material showed a small amount of cyclic hardening but saturation occurred within the first few cycles and a constant stress was maintained throughout the life of the sample. These results are similar to the results observed by Calabrese and Laird (5) in Al-4Cu containing θ' precipitates. Transmission electron microscopy studies of the fatigued composite revealed dislocation structures similar to those previously reported (5). Dislocation accumulation was observed in the matrix between the θ' precipitates and at the precipitate matrix interface. This stable behavior, according to Calabrese and Laird (5), is a result of mobile dislocations shuttling between θ' precipitates accommodating the imposed plastic strain without further hardening. Based upon these observations it may be concluded that the mechanisms governing the cyclic response of the composite appear to be quite similar to those governing unreinforced aluminum.

For the artificially aged microstructure, the loop shape parameter showed no distinct evidence of any minimum. This result may be interpreted based upon the strong particle model proposed by Calabrese and Laird (5) where slip is restricted to shuttling dislocations between the θ' precipitates. Hence, strain localization in the form of PSBs does not occur in these materials and the loop shape parameter remains at a constant value throughout life.

While it is conceivable that cracking early in the fatigue life may influence the cyclic response curve and/or the loop shape parameter, this is not considered to be a significant factor in the present study. Microstructure has been observed to show a negligible influence on the fatigue crack growth rates in a 2124 / SiC composite (15) which suggests that an influence of cracking on the cyclic response and loop shape parameter should also be independent of micro-structure. Since microstructure had a significant influence on both the cyclic response and the loop shape parameter, we conclude that the influence of cracking on these characteristics is minimal.

Due to the cyclic instability of the naturally aged material, plastic strain controlled experiments and load controlled experiments in the low cycle regime yielded dramatically different results when compared on a stress - life curve (Figure 6). For plastic strain-controlled tests, the plastic strain amplitude is held constant and the stress required to produce this plastic strain varied as the material hardens. In contrast, in stress-controlled fatigue tests, the stresses are held constant and the plastic strain required to obtain the desired stress varied as the material hardens. Thus at high stresses, the plastic strain required to accommodate the desired stress is much higher than the plastic strain required to obtain the equivalent saturation stress in a plastic strain-controlled test. As a result, accelerated damage occurs in the first few cycles of a stress-controlled test and hence leads to a shorter fatigue life in the low cycle regime. In contrast, the artificially aged microstructure is cyclically stable and the peak stresses from plastic strain-controlled experiments coincide with those of the load control fatigue experiments. Thus on the stress-life curve, plastic strain controlled testing and load controlled testing were indistinguishable for the artificially aged system. Interestingly, the fatigue life of the composite material did not appear to be dependent upon the precipitate type, i.e. shearable or nonshearable in either stress - controlled or plastic strain controlled testing. Although this is not fully understood, it is similar to recently reported results in a 2014 / Al_2O_3 composite (3).

Despite the markedly different cyclic response of these two microstructural conditions, the plastic strain life and stress life behavior were virtually indistinguishable. The lack of a difference in life of these two microstructures may be related to the initiation of fatigue cracks at intermetallic particles and implies that fatigue crack propagation domin-

ates life at all stress levels. Several investigators have observed that fatigue cracks initiate at such intermetallics (1, 2, 16-18). Given the measured volume fraction of the Al_3Ti intermetallics and their large size, it may be reasonable to assume that these intermetallics may have acted as initiation sites. Scanning electron microscopy of the fatigued samples has, however, failed to provide evidence for this hypothesis. Surface damage from the fully reversed cycling may have obliterated the intermetallics leaving no evidence that they nucleated cracks. The possibility that fatigue life is dominated by fatigue crack propagation in these composite materials is significant and could influence strategies for understanding and further improving the fatigue behavior of particulate reinforced composites.

Conclusions

The influence of matrix microstructure on the cyclic response of an XD™ 2219/15/TiCp composite generally parallels the behavior of unreinforced precipitation-hardened aluminum alloys reported by other investigators. The presence of shearable precipitates produced by natural aging leads to a cyclically unstable microstructure and strain localization. This cyclic response consisted of a rapid hardening region followed by a region where the hardening rate decreases and ultimately a region of cyclic softening. Further, it appears that the loop shape analysis used by other investigators to detect strain localization in single phase materials may be applicable for more complex materials. The presence of nonshearable precipitates produced by artificial aging lead to a cyclically stable structure with no evidence of strain localization. Although precipitate morphology was observed to significantly influence the cyclic response of these composites, it generally had no influence on the fatigue life under either plastic strain-controlled or under stress-controlled fatigue testing.

Acknowledgements

References

1.   J. Van de Polder, Master's Thesis, The University of Michigan, 1988.
2.   J. Bonnen, J. Allison, J. Jones, Met. Trans. 22A, 1007, (1991).
3.   C. Liu and J. Lewandowski, presented at TMS Symposium on "Fatigue and Creep in Metal Matrix Composites", New Orleans, LA, February 1991.
4.   C. Calabrese and C. Laird, Mat. Sci. and Eng. 13, 141, (1974).
5.   C. Calabrese and C. Laird, Mat. Sci. and Eng. 13, 159, (1974).
6.   A. Renard, A. Cheng, R. de la Veaux, and C. Laird, Mat. Sci. and Eng. 60, 113, (1983).
7.   A. R. C. Westwood, Met. Trans. 19B, 155, (1988).
8.   L.A. Willey, ASM Metals Handbook vol. 8, p.387, 8th edition, Metals Park, OH (1973).
9.   H. Mughrabi, Mat. Sci. and Eng. 33, 207, (1978).
10.   D. E. Witmer, C. Laird, and G. C. Farrington, Acta Met. 35, 1911, (1987).
11.   J. Papazian, Met. Trans. 12A, 269, (1981).
12.   T. H. Sanders, J. T. Staley, and D. A. Mauney, Fundamental Aspects of Structural Alloy Design, p. 487, Plenum Press, New York (1975).
13.   M. E. Fine and J. S. Santner, Scripta Met. 9, 1239, (1975).
14.   J. Polak, K. Obrtlik, and J. Helesic, in "Fatigue '90", Eds.: H. Kitagawa and T. Tanaka, Materials and Component Engineering Publications Ltd., Birmingham, UK, 1990, p. 217.
15.   C. P. You and J. E. Allison, in "Advances in Fracture Research (ICF7)", Eds.: K. Salama, K. Ravi-Chandar, D. M. Taplin, and P. Rama Rao, Pergamon Press, Oxford, UK, 1989, p. 3005.
16.   W. L. Morris, O. Buck, and H. L. Marcus, Met. Trans. 7A, 1161, (1976).
17.   W. L. Morris, Met. Trans. 9A, 1345, (1978).
18.   C. Y. Kung and M. E. Fine, Met. Trans. 10A, 603, (1979).